

UKAEA-CCFE-PR(19)47

C. Vincent, W. McCarthy, T. Golfinopoulos, B.
LaBombard, R. Sharples, J. Lovell, G. Naylor, S. Hall,
J. Harrison and A.Q. Kuang

The Digital Mirror Langmuir Probe: FPGA Implementation of Real-Time Langmuir Probe Biasing

Enquiries about copyright and reproduction should in the first instance be addressed to the
UKAEA
Publications Officer, Culham Science Centre, Building K1/0/83 Abingdon, Oxfordshire,
OX14 3DB, UK. The United Kingdom Atomic Energy Authority is the copyright holder.

The Digital Mirror Langmuir Probe: FPGA Implementation of Real-Time Langmuir Probe Biasing

C. Vincent, W. McCarthy, T. Golfinopoulos, B. LaBombard, R.
Sharples, J. Lovell, G. Naylor, S. Hall, J. Harrison and A.Q. Kuang

The Digital Mirror Langmuir Probe: Field Programmable Gate Array Implementation of Real-Time Langmuir Probe Biasing

C. Vincent,^{1,2, a)} W. McCarthy,³ T. Golfinopoulos,³ B. LaBombard,³ R. Sharples,¹ J. Lovell,⁴ G. Naylor,² S. Hall,² J. Harrison,² and A.Q. Kuang³

¹⁾*Department of Physics, Durham University, South Road, Durham, DH1 3LE, UK*

²⁾*United Kingdom Atomic Energy Authority, Culham Centre for Fusion Energy, Culham Science Centre, Abingdon, Oxon, OX14 3DB, UK*

³⁾*Plasma Science and Fusion Centre, Massachusetts Institute of Technology, 77 Massachusetts Avenue, Cambridge, MA 02139, USA*

⁴⁾*Oak Ridge National Laboratory, Oak Ridge, Tennessee 37831, USA*

(Dated: 29 July 2019)

High bandwidth, high spatial resolution measurements of electron temperature, density and plasma potential are valuable for resolving turbulence in the boundary plasma of tokamaks. While conventional Langmuir probes can provide such measurements either their temporal or spatial resolution is limited: the former by the sweep rate necessary for obtaining I-V characteristics and the latter by the need to use multiple electrodes, as is the case in triple and double probe configurations. The Mirror Langmuir Probe (MLP) bias technique overcomes these limitations by rapidly switching the voltage on a single electrode cycling between three bias states, each dynamically optimised for the local plasma conditions. The MLP system on Alcator C-Mod used analog circuitry to perform this function, measuring T_e , V_F , and I_{sat} at 1.1 MSPS. Recently, a new prototype digital MLP controller has been implemented on a Red Pitaya Field Programmable Gate Array (FPGA) board which reproduces the functionality of the original controller and performs all data acquisition. There is also the potential to provide the plasma parameters externally for use with feedback control systems. The use of FPGA technology means the system is readily customisable at a fraction of the development time and implementation cost. A second Red Pitaya was used to test the MLP by simulating the current response of a physical probe using C-Mod experimental measurements. This project is available as a git repository to facilitate extensibility (e.g. real-time control outputs, more voltage states) and scalability through collaboration.

Keywords: Fusion, Plasma, Langmuir probe, Field Programmable Gate Array, Real-time, Koheron, Red Pitaya

I. INTRODUCTION

In order to understand the physics behind plasma transport in the boundary of fusion devices, it is often necessary to have temperature, density, and plasma potential measurements resolved on the time scale of the turbulence driving the transport^{1,2,3}. A scanning Langmuir probe (LP) is a natural choice of diagnostic as it can simultaneously measure all three quantities. However, standard LP biasing techniques are not able to resolve the plasma parameters with sufficient temporal or spatial resolution to observe the fast transport processes. The Mirror Langmuir Probe (MLP) biasing method, first employed on Alcator C-Mod, allows LPs to sample at a much higher bandwidth⁴. By optimising the voltage bias applied to a Langmuir probe based on the real time plasma temperature, the MLP is able to accurately sample plasma parameters at 1.1 MSPS bandwidth. This enabled study of fast edge turbulence and led to improved characterization of the Quasi-Coherent Mode in Alcator C-Mod EDA H-Mode discharges².

The MLP control system used for C-Mod consisted of a complex system of analogue electronic components that made implementation and set up time consuming and increased maintenance difficulty. This paper reports the first prototype of a digital implementation of Langmuir probe bias calculation and switching emulating the behaviour of a Mirror Lang-

muir Probe system. This will reduce the setup time of new systems significantly, as well as improve upgradability, customisability and scalability. Additional electronics will still be needed to drive the physical probe and these will be specific to the plasma device on which the system is implemented.

This paper describes the design and implementation of a prototype digital of the MLP control scheme that we have built. A novel test procedure for the digital MLP is also described using a hardware platform that emulates the plasma current response. We consider this method analogous to synthetic diagnostics used to validate simulations.

II. BACKGROUND

A. The Langmuir Probe I/V Model

A Langmuir probe is a small conductive piece of material that is inserted into a plasma. In a fusion research plasma the probes can generally only be used in the edge region (outside the last closed flux surface) as the high temperatures closer to the core would cause melting or ablation of the probe. Langmuir probes can be used to determine plasma parameters by performing an I-V characteristic reconstruction⁵. The I-V characteristic, shown in figure 1 and expressed in equation 1, is a curve generated by measuring the current response of the probe to a series of applied voltages. The lower portion of the characteristic, in the vicinity of $V_{pr} = V_F$, is then fit to the

^{a)}Electronic mail: charles.h.vincent@durham.ac.uk

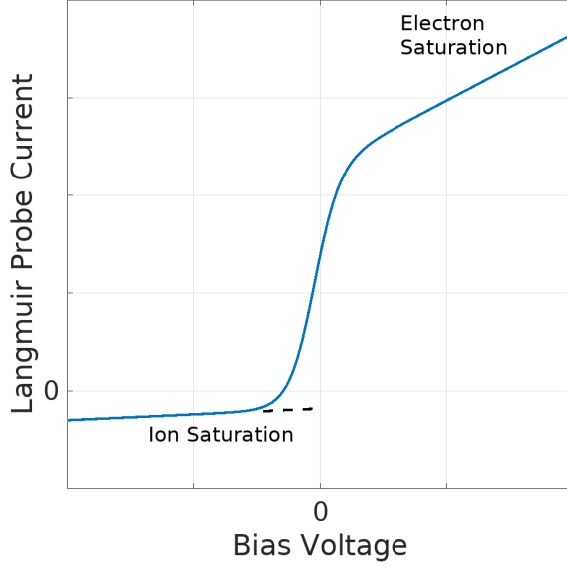


FIG. 1: Diagram showing the I/V characteristic of a Langmuir probe. The slope and current axis intercept, which are used to extract plasma parameters, can shift for a given probe depending on the plasma temperature and floating voltage, as shown in equation 1.

Langmuir Probe equation⁶:

$$I_{LP} = I_{sat} (e^{(V_{pr} - V_F)/T_e} - 1) \quad (1)$$

where I_{LP} is the current collected by the probe, I_{sat} is the ion saturation current, V_F is the floating potential of the probe surface due to the plasma, and V_{pr} is the total bias on the probe. The plasma quantities of temperature T_e , floating voltage V_F , and saturation current I_{sat} are determined by fitting this model function to the measured I-V characteristic.⁶ Since T_e and V_F can vary and are *a priori* unknown, a conventional Langmuir probe control system sweeps the probe voltage V_{pr} over a large range to be sure it obtains a well-conditioned I-V characteristic. Control systems based on this method tend to be slow relative to fast turbulence phenomena⁷ as many data samples must be collected per sweep and subsequently fitted. Alternatively, a double or triple probe configuration could be implemented⁸, but as this makes use of spatially separated probe tips the spatial resolution becomes limited compared to a single probe. By constantly optimising the voltage bias levels relative to the plasma temperature the MLP is able to report fitted parameter data at high speeds using a single electrode.

To maximise the sweep speed, as few points as possible along the I-V curve are measured. The minimum number of voltage states necessary to get an I-V characteristic reconstruction is three (the number of degrees of freedom in the model, with each voltage state corresponding to a sampled point). To capture the physics contained within the characteristic the ion saturation current (I_{sat}), the zero crossing voltage of the current (set by V_F), and the curvature of the I-V characteristic for voltages above V_F (set by T_e) must all be accurately

measured. However, since these quantities change in time, the optimum bias voltages necessary to sample them also changes in time. The aim of the MLP bias approach is to deduce these quantities (I_{sat} , V_F , T_e) dynamically in real-time as the data are collected and adjust the probe bias voltages accordingly. Of these, the most important parameters are T_e and V_F .

The bias control problem can be made somewhat easier by capacitively coupling the probe driver to the probe electrode and insisting on bias states that produce currents of $I_0 = 0$, $I_+ = I_{sat}$, $I_- = -I_{sat}$. If these conditions are upheld, the time-average current over the capacitor will be zero and it will charge to the floating potential, if the amplitudes of the positive and negative biases are suitably chosen. This allows the applied bias voltage, driven by an external voltage source, to be relative to the floating potential.

The desired applied bias voltages that accomplish this can be found by simultaneously solving the LP equation near $I = I_{sat}$ and $I = -I_{sat}$ and requiring that the difference between them be 4 times T_e . This bias range insures that a complete I-V characteristic will be sampled and appropriately adjusted as T_e changes. The resulting non zero applied biases sit on top of the capacitor bias, which should be approximately V_F , and are given in terms of electron temperature as:

$$\begin{aligned} V_- &= -3.325T_e \\ V_+ &= 0.675T_e \end{aligned} \quad (2)$$

The total probe bias is given by:

$$V_{pr} = V_{\pm,0} + V_C \quad (3)$$

where $V_{\pm,0}$ are the externally applied driving bias and V_C is the voltage across the capacitor (ideally the floating potential). The total probe bias is what is usually measured in experiment. Capacitor bias can be inferred from the difference in the known externally controlled drive and the measured total bias.

The current collected in the V_- bias state is bounded by the value $I = I_{sat}$, and because the range of times T_e , is more-or-less guaranteed to be very close to this value. The chosen value of V_- then constrains the value of V_+ such that $I_- = I_+$ and the current through the coupling capacitor is averaged to zero⁴.

Fitting algorithms are too slow to allow a real-time calculation of T_e so the new MLP controller attempts to calculate the plasma temperature in real time using an alternative algorithmic approach⁴. At each of the three bias states, the value of one of the plasma parameters is updated. The calculations are performed in terms of the total probe bias (applied plus capacitor), current, and old plasma parameters.

- The negative applied bias (V_-) is assumed to be sufficiently negative such that the probe is collecting the ion saturation current. The rearranged Langmuir probe equation provides a small correction and is shown in equation 4.

$$I_{sat} = I_{LP} / \left(\exp\left(\frac{V_P - V_F}{T_e}\right) - 1 \right) \quad (4)$$

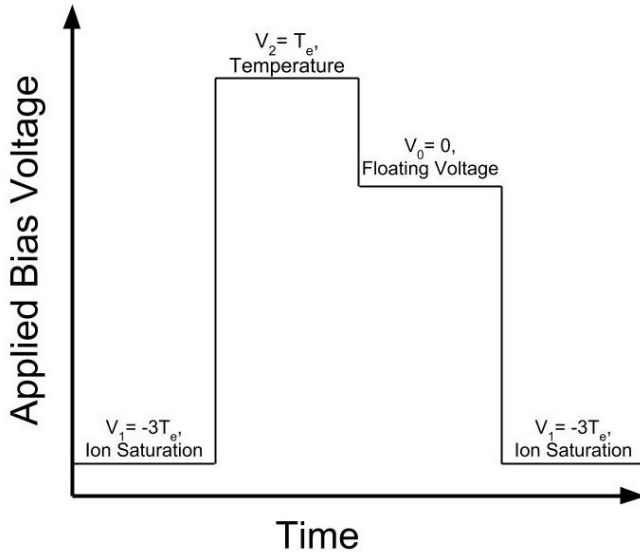


FIG. 2: Diagram of the bias state order for the MLP and the value calculated at each state. The startup state is the positive voltage and a new temperature is calculated at the end of this bias state, to be applied at the negative voltage state. For an ideal system values of $-3.325T_e$ and $0.675T_e$ would be used, but for simplicity rounded values have been used for the prototype.

- The positive applied bias (V_+) is used to calculate the electron temperature. The rearranged Langmuir probe equation is shown in equation 5.

$$T_e = (V_{pr} - V_F) / \ln\left(\frac{I_{LP}}{I_{sat}} + 1\right) \quad (5)$$

- The final bias state places the applied bias to the probe to zero volts. At this voltage the current to the probe should be close to zero. A residual current means that the charge on the capacitor is not quite equal to the floating potential. V_F is computed using the rearranged Langmuir probe equation shown in equation 6.

$$V_F = V_P - T_e \ln\left(\frac{I_{LP}}{I_{sat}} + 1\right) \quad (6)$$

The bias state order is demonstrated in figure 2. It is worth noting that the original MLP did not explicitly implement these equations. Instead analogue electronics were used to mirror a probe response and thus implicitly implemented the equations⁴ by generating a mirrored I-V characteristic from high frequency bipolar transistors and high bandwidth operational amplifiers⁴. When explicitly implementing these equations using digital electronics care must be taken to assure that the algorithm converges to produce stable bias state values. In the following sections we discuss explicit implementation of these equations in digital electronics.

B. Field Programmable Gate Arrays and the Koheron SDK

Field Programmable Gate Arrays (FPGAs) are reconfigurable integrated circuits. This makes them extremely useful for research where it is often necessary to develop new signal processing instrumentation which may need to change over time.

This project uses Red Pitaya FPGA boards⁹. The Red Pitaya boards use a Zynq 7010 SoC (System-on-Chip) with 512MB of RAM and an embedded dual-core ARM processor. This development board is particularly useful for signal processing applications as it incorporates two 125 MSPS Analogue-to-Digital converters (ADCs) and two 125 MSPS Digital-to-Analogue converters (DACs).

Facilitating communication between the ARM processor and the FPGA logic is the Koheron software development kit (SDK)¹⁰. The Koheron SDK is a software development kit for several Zynq 7000-based FPGA boards and provides basic instruments, which can be adapted for most purposes, with the requisite firmware, software and Python libraries necessary for control already pre-installed. This significantly reduces the amount of time it would usually take to develop an instrument, as well as abstracting control to Python, making it easier for collaborators to use in the future.

III. IMPLEMENTATION OF THE DIGITAL CONTROL SYSTEM

A. The Mirror Langmuir Probe Control System

The MLP control system is implemented using a Red Pitaya FPGA board. Current sampling and bias state calculation are accomplished on the FPGA chip while system configuration and data storage utilizes C++ and Python code running on the ARM processor. As stated above, communication between the ARM processing system and FPGA is handled through libraries provided by the Koheron SDK. Interface with the ADCs and DACs on the Red Pitaya is handled by an imported module from the Koheron SDK. The calculation modules are triggered once for each bias state.

Digital electronics are well-suited to additions, subtractions and multiplications while divisions and more complicated operations like the exponentials and logarithms found in equations 2, 3 and 4 are difficult and resource-intensive to implement. Xilinx provides a module to calculate divisions but there is no module to calculate an exponent or logarithm. Instead, look-up tables have been generated for each exponential term where values outside the boundaries of the look-up tables are set to a standard value.

B. The Plasma Current Response System

In order to test the MLP FPGA controller in a controlled and reproducible manner, a second Red Pitaya was used to create a synthetic Plasma Current Response (PCR). The PCR

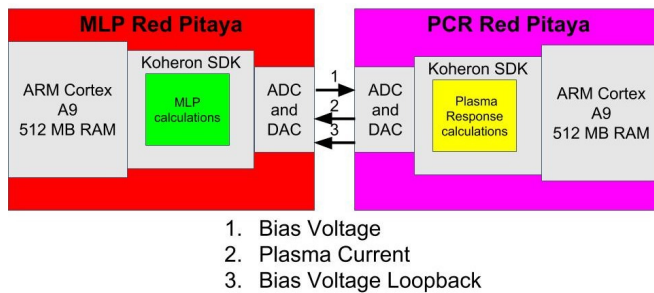


FIG. 3: Cartoon of the Mirror Langmuir Probe and Plasma Current Response instruments connected in "duelling" mode.

The cartoon also shows the components in a Red Pitaya system, with the Koheron SDK handling communication between the FPGA (in green and yellow) and the processing system

is given time series profiles of the plasma parameters and, taking a bias voltage (from the MLP) as input, produces a value of the probe current as output, according to the LP equation constrained by the input profiles. This configuration is shown in figure 3, in what we have chosen to call "duelling" mode, demonstrating the back and forth of the PCR and MLP as each calculates the appropriate response to an applied voltage. It is desirable for the MLP controller to be agnostic to the "plasma" it is connected to, and so the PCR was designed to be completely independent of the MLP except for returning the values the MLP would receive from a real probe in plasma. In contrast to the MLP, the PCR runs a calculation stream so that each input sample has a corresponding output sample and it is therefore independent of MLP triggering. The programmability of the Koheron SDK means arbitrary or non-realistic plasma parameters may be set for diagnostic purposes, as well as allowing for more complex models and real data streams to be used to benchmark Langmuir probe control systems.

During these tests there was no capacitive coupling between the MLP and PCR FPGA boards. As such the applied bias becomes the full probe bias. The effect of this on the algorithm can be seen by setting V_C equal to zero in equation 3. These modified equations were what was programmed into both the MLP and PCR FPGA boards. Any future real plasma tests will include capacitive coupling and use the full forms of the equations.

C. Hardware and Digitisation

The test setup consists of two Red Pitaya (RP) boards connected together with SMA cables, as shown in figure 3, using the 125 MSPS ADCs and DACs integrated into the Red Pitaya board. Each input is terminated with 50Ω to reduce reflections of the high speed switch signal, which would otherwise lead to inaccurate sampling of the input voltages.

Digitisation of the data is performed by the RP MLP. The MLP includes modules for input calibration and input smoothing, though smoothing of the incoming signal was found to be

unnecessary for our test cases. The PCR calculates the plasma current for a given input bias voltage, and then outputs the calculated current and the probe voltage. These signals are then processed by the MLP using digital filters and used to calculate the plasma parameters and set the bias states for the next voltage cycle. At each bias state, five measurements of the applied bias and the returned current from the PCR are recorded at equally-spaced intervals. Only the final measurement is used to calculate the next bias state with the previous values used in post-processing to confirm that the applied voltage has settled. The calculated temperature, current and floating potential are stored each time a new temperature is calculated.

A basic calibration module is currently implemented within the test system. By looping the voltage out of the MLP back into the control system the offset and scaling factor can be measured. These are then programmed into the control system using the python interface to be applied to the incoming signal before the bias calculation modules.

A limitation of this first generation system is demonstrated in figure 6 where the ratio V_+ to V_- is different to that given by the values in equation 2. This is due to the quantisation of values necessary when using digital electronics. This has resulted in the use of 1 and -3 times T_e instead of 0.625 and -3.325 for the positive and negative bias'. However, this does not seem to have effected performance greatly as shown by the various figures in section IV where the calculated temperatures still trace the input temperatures well.

IV. MLP EMULATION

This project has reproduced chief performance objectives (such as temperature calculation and real-time bias adjustments) in synthetic tests and therefore is shown to emulate the original MLP system with our current test setup. Three tests were used to confirm that the MLP was operating correctly. A step test in temperature confirms that bias values are adjusted correctly and triangular waveforms (of the artificial plasma temperature) show that the MLP can follow variations in plasma parameters. Finally the MLP is tested against real data from past C-Mod shots to compare its accuracy against the analogue system.

A. Temperature Step Change

The core feature of the MLP control system is that it can change bias states in real-time according to the plasma temperature. Figure 4 gives a demonstration of how the MLP calculates a step change in temperature (shown in red). The calculation time for a step change in temperature is equivalent to one full bias cycle, which in this case is approximately $3 \mu s$. The application of a temperature step change also shows a systematic overestimation in the MLP temperature calculation, which varies between 10% and 20%. This does not seem to affect the post-process parameter fitting however (a calibra-

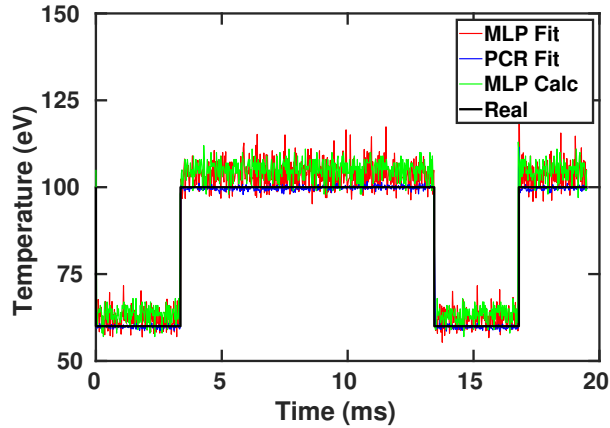


FIG. 4: This figure shows the response of the MLP control system to a step change in temperature from 60eV to 100eV. While the MLP systematically overestimates the temperature, the response is close to instantaneous.

tion error has caused the offset in figure 4), as the corresponding currents are measured correctly (shown in blue).

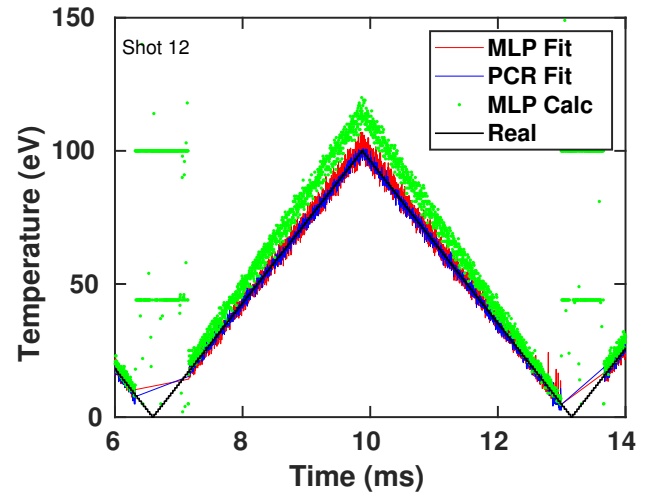
B. Triangular Waveforms

Figure 5a shows that the MLP can follow a triangular waveform for the majority of the range from 0 eV to 100 eV. The same can be seen for the floating potential, as shown in figure 5b, and the resulting bias states, as shown in figure 6. These figures show that the MLP system can quickly react to changes in the plasma parameters simulated by the PCR system. In figures 5a and 5b the MLP was operating at a cycle speed of 1 MHz. A deficiency of the test system is demonstrated in figures 5a and 5b as failure to calculate plasma parameters for $T_e < 15\text{eV}$ consistently. This is due to the PCR calculations diverging at low temperatures and outputting a non-physical plasma current. The LP equation exponential is calculated using a preloaded look-up table, so when T_e is small the values of the argument of the exponential may go out of the range covered by the look-up table. This makes a fit impossible and causes the MLP parameter calculation to become volatile.

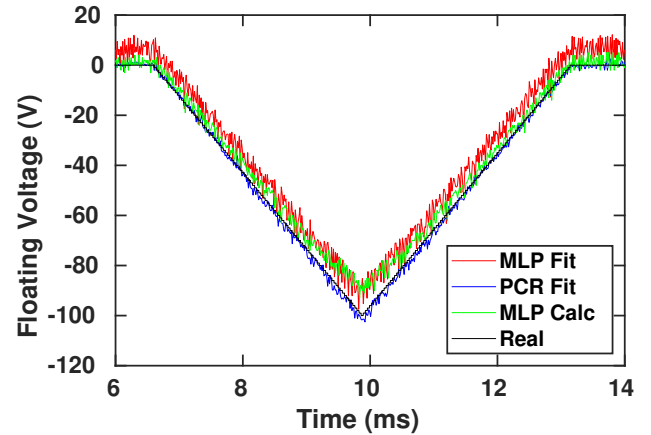
Beyond 1 MSPS the settling time of the RP DACs and the latency of the PCR calculations limit performance. At a full rate of 320 ns per bias state (compared to $1\mu\text{s}$ in figure 4), the PCR latency (240 ns) is a significant proportion of the bias state time. This means that the sampled current is mismatched to the applied voltage, and as a proportion of the sampling takes place during the 50 ns settling time of the DAC the current is not well-defined.

C. Tests With C-Mod Data

In the final test performed on the MLP controller, we provided the PCR with time series data (in T_e , I_{sat} and V_F) taken from operation of the C-Mod MLP. The C-Mod data was taken



(a) The MLP response to a triangle waveform change in temperature.



(b) The MLP response to a triangle waveform change in floating potential.

FIG. 5: These figures demonstrate the calculated change in temperature and plasma potential for a triangle waveform. 5a shows the response of the MLP control system to a triangular change in temperature and 5b shows the response to a triangular change in plasma potential. While they demonstrate that the trend is followed well they also expose the inability to calculate low temperatures ($< 15\text{eV}$).

at a sampling rate of 1 MSPS, however for this test it was artificially slowed down by a factor of two to account for the PCR latency. The results of this test are shown in figure 7. It is immediately clear looking at the figure that large plasma fluctuations are present in the C-Mod MLP data. For most of this time-window, the real-time calculations (shown in green) track the real data well, only deviating by a few electron volts in several places. The post-processed plasma parameters (shown in red) match even more closely and the error seen is well below the 10% error normally associated with normal Langmuir probe operation. A $100\text{-}\mu\text{s}$ window is expanded in the inset figure, and individual points are shown to demonstrate the ability of the MLP to resolve real plasma

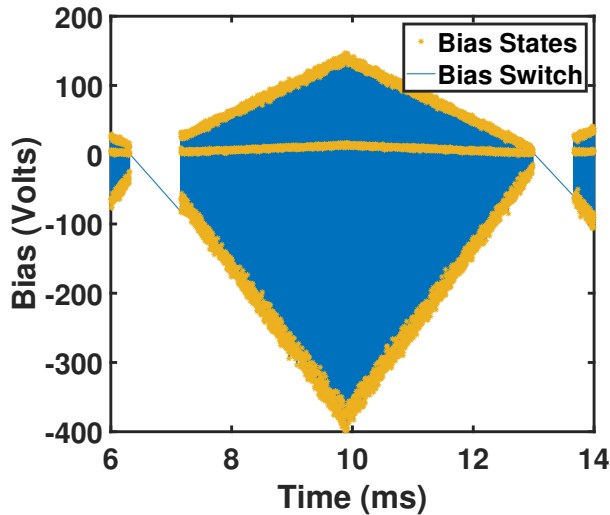


FIG. 6: The bias state overlays for the triangle waveform shown in 5a. The blue line approximates the probe output voltages and appears as a blue block due to the high speed switching of the probe. The yellow shows the average probe voltage at each stable bias state and so approximates V_+ , V_F and V_- . When the calculation fails the bias states will revert to a standard value.

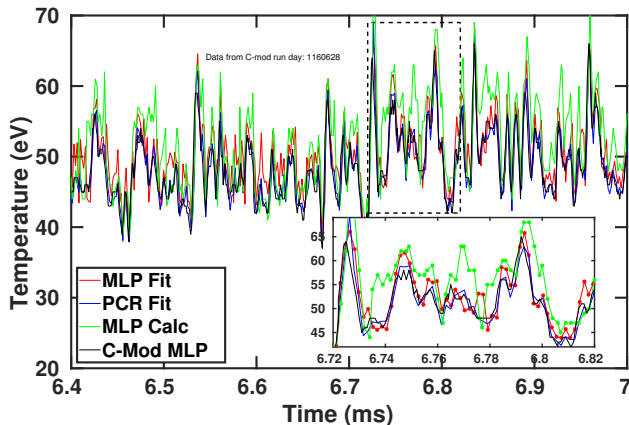


FIG. 7: A demonstration of real C-Mod turbulence data fed to the PCR module. The MLP appears to follow the turbulence well enough to allow an accurate post-processing fit of plasma parameters, as demonstrated by the inset.

fluctuations. This demonstration shows that the digital MLP controller is able to replicate the C-Mod MLP ability to resolve real plasma turbulence.

V. FURTHER WORK

We have now demonstrated the viability of a digital Langmuir probe control scheme that can adjust bias states in real-time with respect to a fluctuating temperature. Future studies

will include testing on the linear plasma device DIONISOS, at the MIT Plasma Science and Fusion Center¹¹. These tests will be conducted by the team at PSFC and will work to refine device operation and further show the digital MLP viability. In parallel, a PhD student as part of a Centre for Doctoral Training in Fusion will develop the MLP for operation on MAST-U.

Full implementation on fusion experiments will require power electronics to bias the Langmuir probe. As the switching speed is very fast, capacitance due to the cabling will become significant. Minimising the capacitance to retain high bandwidth measurements in a full system is a non-trivial task. The bias algorithm could also be applied to future conventional Langmuir probe control systems¹², making them more information-efficient as they would be able to adjust their temperature sweep according to real-time plasma conditions but also provide real-time plasma parameter signals to other control systems.

VI. SUMMARY

Our tests show that it is possible to implement an MLP control scheme in digital electronics. This significantly improves portability and drastically reduces the time commitment needed for implementation of an MLP system. This new system also gives much greater scope for customisation, with the difficulties of reproduction and maintenance reduced thanks to the standardized FPGA development board and publicly available GitHub repository¹³. The incorporation of Python (thanks to the Koheron SDK) also improves usability.

Testing has shown that the MLP can calculate changes in both temperature and floating potential and then make the necessary changes to the applied bias states. This demonstration has laid the groundwork for future customisable, reproducible and maintainable MLP solutions to be developed independently for different plasma devices. This will significantly improve future studies of fast transport phenomena in the fusion plasma edge².

ACKNOWLEDGEMENTS

This work was supported by the Massachusetts Institute of Technology (supported by US DoE cooperative agreement DE-SC0014264), and by the Engineering and Physical Sciences Research Council (EP/L01663X/1). This work has been carried out within the framework of the EUROfusion Consortium and has received funding from the Euratom research and training programme 2014-2018 and 2019-2020 under grant agreement No 633053. The views and opinions expressed herein do not necessarily reflect those of the European Commission

¹N. Smick and B. LaBombard, “Wall scanning probe for high-field plasma measurements on Alcator C-Mod,” *Review of Scientific Instruments* **80**, 023502 (2009).

²B. LaBombard, T. Golfinopoulos, J. L. Terry, D. Brunner, E. Davis, M. Greenwald, and J. W. Hughes, “New insights on boundary

- plasma turbulence and the quasi-coherent mode in Alcator C-Mod using a Mirror Langmuir Probe,” *Physics of Plasmas* **21**, 056108 (2014), <https://doi.org/10.1063/1.4873918>.
- ³P. W. Terry, “Suppression of turbulence and transport by sheared flow,” *Rev. Mod. Phys.* **72**, 109–165 (2000).
- ⁴B. LaBombard and L. Lyons, “Mirror Langmuir probe: A technique for real-time measurement of magnetized plasma conditions using a single Langmuir electrode,” *Review of Scientific Instruments* **78**, 073501 (2007), <https://doi.org/10.1063/1.2754392>.
- ⁵H. M. Mott-Smith and I. Langmuir, “The Theory of Collectors in Gaseous Discharges,” *Phys. Rev.* **28**, 727–763 (1926).
- ⁶P. Stangeby, *The Plasma Boundary of Magnetic Fusion Devices* (CRC Press, 2000).
- ⁷A. Kirk, A. J. Thornton, J. R. Harrison, F. Militello, N. R. Walkden, the MAST Team, and the EUROfusion MST1 Team, “L-mode filament characteristics on MAST as a function of plasma current measured using visible imaging,” *Plasma Physics and Controlled Fusion* **58**, 085008 (2016).
- ⁸S. Chen and T. Sekiguchi, “Instantaneous Direct-Display System of Plasma Parameters by Means of Triple Probe,” *Journal of Applied Physics* **36**, 2363–2375 (1965), <https://doi.org/10.1063/1.1714492>.
- ⁹“Red Pitaya Organisation,” <https://www.redpitaya.com/> (2018), accessed: 29 July 2019.
- ¹⁰“Koheron SDK,” <https://www.koheron.com/software-development-kit>, accessed: 29 July 2019.
- ¹¹F. Bedoya, K. B. Woller, and D. G. Whyte, “Study of the properties of thin Li films and their relationship with He plasmas using ion beam analysis in the DIONISOS experiment,” *Review of Scientific Instruments* **89**, 10J106 (2018), <https://doi.org/10.1063/1.5034240>.
- ¹²J. Lovell, R. Stephen, S. Bray, G. Naylor, S. Elmore, H. Willett, M. Peterka, M. Dimitrova, A. Havranek, M. Hron, and R. Sharples, “A compact, smart Langmuir Probe control module for MAST-Upgrade,” *Journal of Instrumentation* **12**, C11008 (2017).
- ¹³“Mirror Langmuir Probe GitHub repository,” <https://github.com/Rondin119/MIT-Mirror-Langmuir-Probe> (2019), accessed: 29 July 2019.